LETTERS

Deep origin and hot melting of an Archaean orogenic peridotite massif in Norway

Dirk Spengler[1], Herman L. M. van Roermund[1], Martyn R. Drury[1], Luisa Ottolini[2], Paul R. D. Mason[1] & Gareth R. Davies[3]

The buoyancy and strength of sub-continental lithospheric mantle is thought to protect the oldest continental crust (cratons) from destruction by plate tectonic processes. The exact origin of the lithosphere below cratons is controversial, but seems clearly to be a residue remaining after the extraction of large amounts of melt[1,2]. Models to explain highly melt-depleted but garnet-bearing rock compositions require multi-stage processes with garnet and clinopyroxene possibly of secondary origin[1,3]. Here we report on orogenic peridotites (fragments of cratonic mantle incorporated into the crust during continent-continent plate collision[4]) from Otrøy, western Norway. We show that the peridotites underwent extensive melting during upwelling from depths of 350 kilometres or more, forming a garnet-bearing cratonic root in a single melting event. These peridotites appear to be the residue after Archaean aluminium depleted komatiite magmatism.

The discovery of microdiamonds in both orogenic peridotite and associated subducted crustal rocks in the Western Gneiss Region of Norway implies that both rock suites had a shared evolution during the Scandian orogeny 420–390 million years ago; when the Baltic continental crust was subducted into the diamond stability field (≥120 km)[5–7]. However, the occurrence of pyroxene exsolution in subcontinental lithospheric mantle (SCLM) garnet after majorite indicates a deeper origin for the Western Gneiss Region peridotites (180–250 km)[8,9] than for the surrounding crustal gneisses. Similar significant pressure differences occur in the Dabieshan-Sulu orogen, eastern China[10] and the northern Tibetan plateau[11]. Determining whether the majoritic ultrahigh-pressure microstructure originated before, or during, the Scandian orogeny has major consequences for the geodynamic interpretation[6,8,12]. Here we demonstrate that the exsolution from majorite in the Otrøy peridotites is unrelated to the continental collision that brought the ultrahigh-pressure rocks to the surface.

The Ugelvik peridotite body on Otrøy Island is compositionally layered, comprising garnet-harzburgite and garnet-dunite (~65%), spinel-harzburgite and spinel-dunite (~33%) and minor amounts of garnet-pyroxenite and garnet-websterite layers (<2%)[12,13]. Garnet-bearing layers contain typically 5–10% modal garnet, increasing locally up to 20%. Some layers of garnet-harzburgite and garnet-dunite contain isolated lenses of garnet-websterite[14] (≤45 cm) and garnetite[8] (≤25 cm in diameter). The term nodule is used for centimetre-scale polycrystalline garnet. Previously studied garnetite and garnet nodules[8,9,15] contain pyroxene in two textural positions: grains of orthopyroxene (and rare olivine) in between garnet grains and needles of orthopyroxene (and minor clinopyroxene) in garnet cores, exemplified by sample DS0297 (Fig. 1a–d). Crystallographically oriented intracrystalline pyroxene has been accepted to be of exsolution origin from majoritic garnet[16]. Ugelvik garnetite DS0298

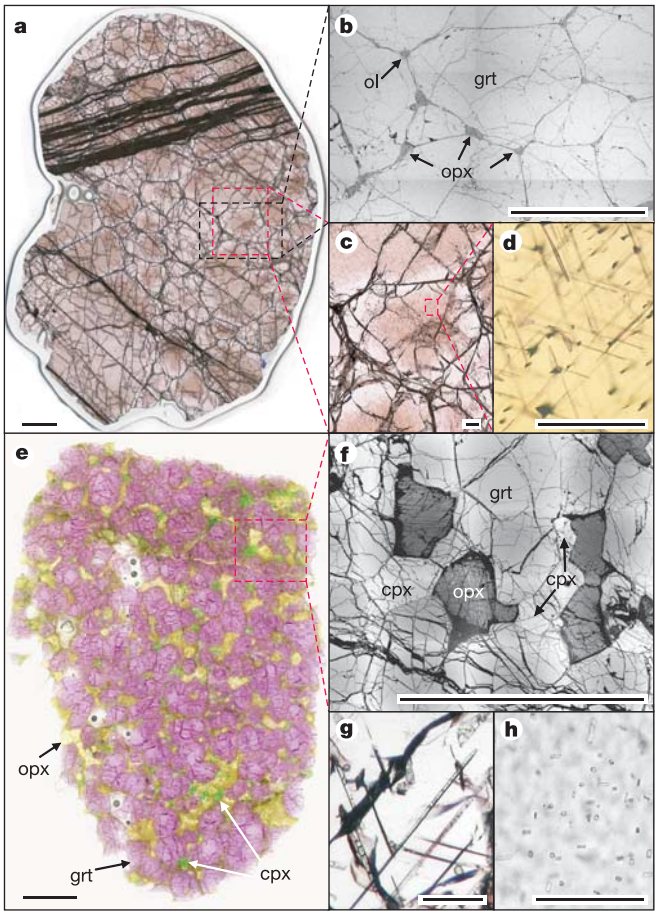

Figure 1 | Photomicrographs showing exsolved inter- and intracrystalline pyroxene within polycrystalline garnetites. a–d, Olivine-bearing garnetite DS0297 represents a well-described microstructure[8,9,15] showing a mosaic garnet texture (**a**) with intercrystalline orthopyroxene and minor olivine (Mg# = 95.0) between individual garnet grains (**b**), crystallographically oriented, prismatic intracrystalline pyroxene needles in garnet cores (**c**, **d**) and needle-free garnet rims (**c**). **e–h**, Olivine-absent garnetite DS0298 differs with intercrystalline ortho- and clinopyroxene between individual garnet grains (**e**, **f**) and with intracrystalline pyroxene precipitates decreasing in size with the garnet grain size (**g**, **h**) in the garnet cores. **a**, **e**, Transmitted light; **c**, **d**, **g**, **h**, plane-polarized transmitted light; **b**, **f**, composite back-scattered electron image. Scale bars in **a**, **b**, **e** and **f** are 1 cm; in **c**, **d**, **g** and **h** they are 500 μm. grt, garnet; opx, orthopyroxene; cpx, clinopyroxene; ol, olivine.

[1]Faculteit Geowetenschappen, Universiteit Utrecht, Budapestlaan 4, 3584CD Utrecht, The Netherlands. [2]Consiglio Nazionale delle Ricerche, Istituto di Geoscienze e Georisorse (IGG)-Sede di Pavia, Via Ferrata 1, 27100 Pavia, Italy. [3]Faculteit der Aard- en Levenswetenschappen, Vrije Universiteit Amsterdam, De Boelelaan 1085, 1081HV Amsterdam, The Netherlands.

(Fig. 1e–h) differs in that it contains clino- and orthopyroxene, but no olivine, at intercrystalline positions. Intercrystalline pyroxene represents >20.6 vol% (Fig. 1e) with a orthopyroxene:clinopyroxene ratio of 4:1. If both inter- and intracrystalline pyroxenes were originally incorporated in the garnet structure, this rock must be derived from close to the Mantle Transition Zone (410–670 km).

To demonstrate that the garnetites were exhumed from this extraordinary depth we must establish that all pyroxene is cogenetic and not a result of an open system process such as melt addition. That all garnetite minerals are extremely depleted in light rare earth elements (REE) (Table 1 and Fig. 2b with chondrite-normalized Ce/Sm < 0.08) clearly demonstrates that no pyroxenes were in contact with a metasomatizing melt or fluid, nor were they crystallized directly from a melt—such processes would produce significantly less light-REE depletion[17]. The pyroxenes have inherited their light-REE-depleted character from the majoritic precursor. This conclusion is supported by the contrasting REE composition of clinopyroxene in a garnet-websterite lens (Fig. 2a), which occurs in the same peridotite body but is interpreted to be of melt origin[6,14].

A high-temperature exsolution origin of all clinopyroxene is suggested by intermineral REE partitioning. The equilibrium REE partitioning between garnet and clinopyroxene is strongly dependent upon atomic number, pressure and temperature[18,19], with a difference of about one order of magnitude in light REE between high and low temperatures[18] (Fig. 2c). Analysed clinopyroxene in this work has Ce contents 8–13 times that of the host garnet. These values are at the high-temperature extreme of both high-temperature/high-pressure mineral partitioning experiments[20] and high-temperature (≤1,380 °C) peridotite xenoliths[18] (Fig. 2a, c). The light-REE partition between garnet and clinopyroxene of both microstructures (inter- and intracrystalline, for the latter an exsolution origin seems indisputable) indicates very high-temperature equilibration, ≥1,300 °C.

Further support for an exsolution origin of intercrystalline pyroxene is provided by decompression experiments on garnet lherzolite performed up to 14 GPa that produced intercrystalline exsolved pyroxene and olivine from majoritic garnet[15]. We therefore conclude, on the basis of the chemistry and microstructure, that the intergrowth of clino- and orthopyroxene was exsolved at high-temperature (≥1,300 °C) from a majoritic garnet precursor. Recalculated precursor garnet compositions from the clinopyroxene-rich garnetite contains >19 mol% majorite (>3.19 silicon cations per formula unit at 12 oxygens), indicating that this garnet was stable at minimum (temperature-dependent) confining pressures of ≥11.5 GPa (refs 21, 22) corresponding to ≥350 km depth (Fig. 3).

Garnet nodules in harzburgite and dunite also constrain the melting history. Nodule DS0213 (~2 cm across) has garnet with millimetre-scale orthopyroxene inclusions. Garnet in nodule DS0289 (~5 cm) contains relicts of intracrystalline pyroxene needles, comparable to the microstructures in the larger garnetite samples. The two garnets are similar in colour and major element chemistry to garnet from the studied garnetites (Supplementary Table 1) except for higher Cr and lower Al. The nodular garnets are characterized by extremely depleted middle REE and exceptionally strongly fractionated heavy REE with chondrite-normalized Dy/Yb < 0.07 (Table 1, Fig. 2b). Garnet is the only significant REE-bearing phase in the garnet-harzburgites and garnet-dunites, and so garnet REE compositions mimic the whole rock.

Such a light-REE-depleted and fractionated-heavy-REE nature can only be explained by large degrees of melt extraction in the garnet stability field, ≥30% (refs 23, 24). This conclusion is consistent with the high Mg# (= Mg/(Mg + Fe)) in olivine from both garnet-bearing and garnet-free harzburgites and dunites, with maxima of

Table 1 | Mineral REE data

Sample	DS0297		DS0297		DS0298		DS0298	
Mineral	Core garnet†		Intracrystalline clinopyroxene†		Core garnet†		Intracrystalline clinopyroxene†	
	Average (*n* = 3)	**s.d.**	**Average (*n* = 9)**	**s.d.**	**Average (*n* = 5)**	**s.d.**	**Average (*n* = 4)**	**s.d.**
La	0.001	0.001	0.052	0.014	0.002	0.002	0.017	0.006
Ce	0.009	0.002	0.15	0.05	0.005	0.004	0.061	0.027
Pr	NA	NA	NA	NA	NA	NA	NA	NA
Nd	0.09	0.03	0.40	0.07	0.030	0.004	0.25	0.11
Sm	0.22	0.05	0.50	0.03	0.07	0.02	0.28	0.13
Eu	0.15	0.02	0.33	0.05	0.09	0.02	0.18	0.04
Gd	0.80	0.08	0.62	0.04	0.65	0.04	0.33	0.08
Dy	2.57	0.35	0.40	0.03	2.26	0.13	0.44	0.06
Y	19.85	0.36	2.01	0.09	17.91	0.14	2.49	0.37
Er	3.05	0.25	0.18	0.02	2.55	0.13	0.20	0.01
Yb	4.39	0.22	0.17	0.03	3.30	0.09	0.27	0.01

Sample	DS0298		DS0298		DS0213		DS0289	
Mineral	Core garnet‡		Intercrystalline clinopyroxene‡		Matrix garnet‡		Matrix garnet‡	
	Average (*n* = 16)	**s.d.**	**Average (*n* = 8)**	**s.d.**	**Average (*n* = 7)**	**s.d.**	**Average (*n* = 10)**	**s.d.**
La	BD	BD	0.014	0.005	0.012	0.005	0.007	0.002
Ce	0.004	0.001	0.034	0.007	0.13	0.02	0.010	0.003
Pr	0.002	0.001	0.012	0.002	0.029	0.005	0.004	0.0005
Nd	0.05	0.01	0.14	0.01	0.11	0.03	0.046	0.012
Sm	0.09	0.02	0.26	0.02	0.031	0.009	0.033	0.008
Eu	0.08	0.02	0.13	0.01	0.011	0.004	0.010	0.002
Gd	0.59	0.07	0.43	0.04	0.023	0.004	0.035	0.007
Dy	2.23	0.14	0.45	0.02	0.059	0.014	0.091	0.009
Y	18.91	1.23	2.09	0.17	1.37	0.07	1.73	0.07
Er	2.43	0.19	0.18	0.02	0.23	0.02	0.29	0.03
Yb	3.45	0.22	0.11	0.03	0.75	0.09	0.89	0.05

Average REE data for garnet and intra- and inter-crystalline clinopyroxene with concentrations in p.p.m. and s.d. of 1σ.
†Analysed by SIMS; ‡analysed by LA-ICP-MS. NA, not analysed; BD, below detection.

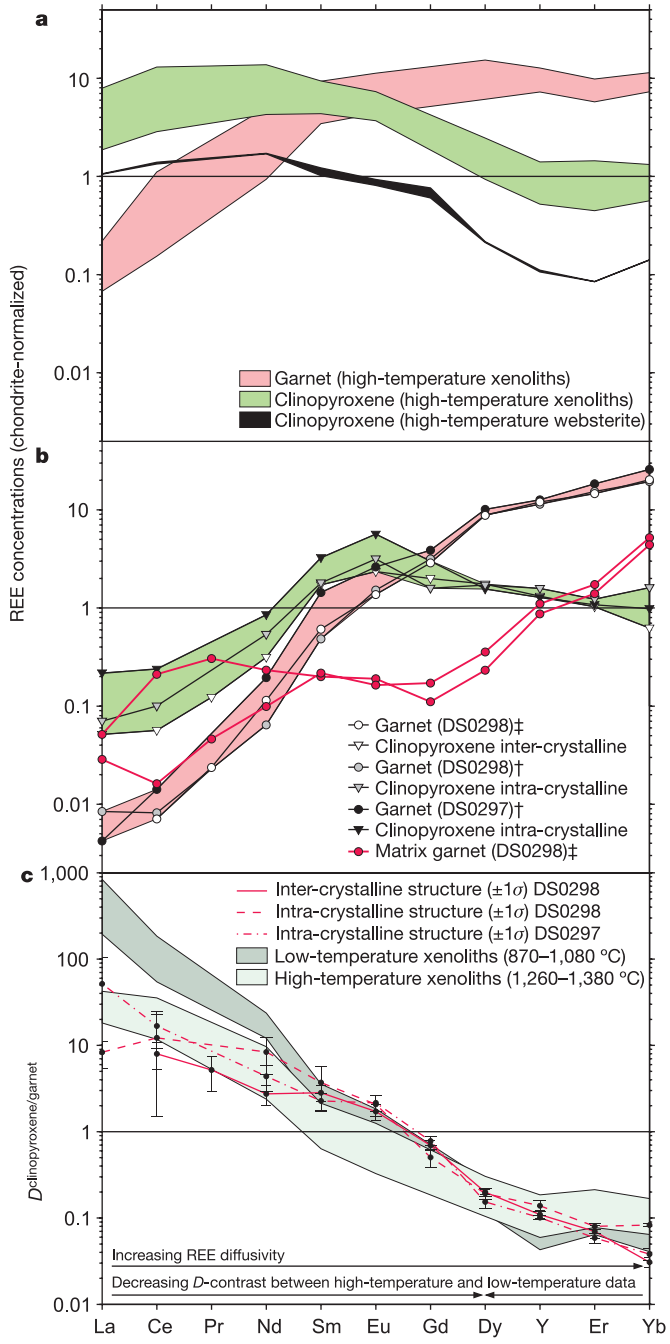

Figure 2 | C1-chondrite normalized mineral REE data from mantle xenoliths and Otrøy orogenic peridotites. **a**, Mineral REE concentrations from high-temperature xenoliths thought to be in chemical equilibrium[18] and from a garnet-websterite lens on Otrøy, interpreted to be crystallized from a melt[6,14]. Clinopyroxenes show elevated abundances of light REE. **b**, Mineral REE concentrations from Otrøy garnetites (shaded) and matrix garnets (red lines). All garnetite minerals show strongly depleted light REE (those analysed by SIMS marked with a dagger; those analysed by LA-ICP-MS marked with a double dagger) and contrast with nodular matrix garnet, which records even stronger depletion in middle REE and exceptionally fractionated heavy REE. **c**, Clinopyroxene–garnet REE partition coefficients *D* in Otrøy garnetites in comparison with those from high-temperature and low-temperature xenoliths[18]. Light REE in this study show a high-temperature equilibration, whereas middle and heavy REE indicate a low-temperature partitioning. The low-temperature REE partitioning is consistent with a re-equilibration during cooling below 1,100 °C over an appropriate time span because experimentally determined diffusion rates are faster for middle and heavy REE than for light REE[19].

0.926–0.930 (refs 25, 32). Together, these data require the onset of melting during decompression at ≥1,800 °C and ≥8 GPa (Fig. 3), otherwise garnet melts completely before olivine reaches these Mg#. Such high temperatures of melting only existed in the Archaean era[25,26,32].

Nd isotope ratios were determined to constrain the time of melting and cooling of the peridotites (Supplementary Table 2). Intercrystalline clinopyroxene and garnet in sample DS0298 define a mid-Proterozoic cooling age of 1.4 billion years (Gyr) before present (BP) (Supplementary Fig. 1). The 1.4 Gyr BP age establishes that intercrystalline pyroxene exsolution within the garnetite occurred long before the Scandian orogeny. Comparable REE partitioning between both intra- and intercrystalline pyroxene and garnet show that exsolution occurred at high temperature (>1,300 °C). We therefore disagree with previous suggestions that the Caledonian continental subduction was responsible for all decompression textures in the garnet peridotites[6]. Consequently we favour a multistage exhumation history[8,27]. It follows that the occurrence of ultrahigh-pressure

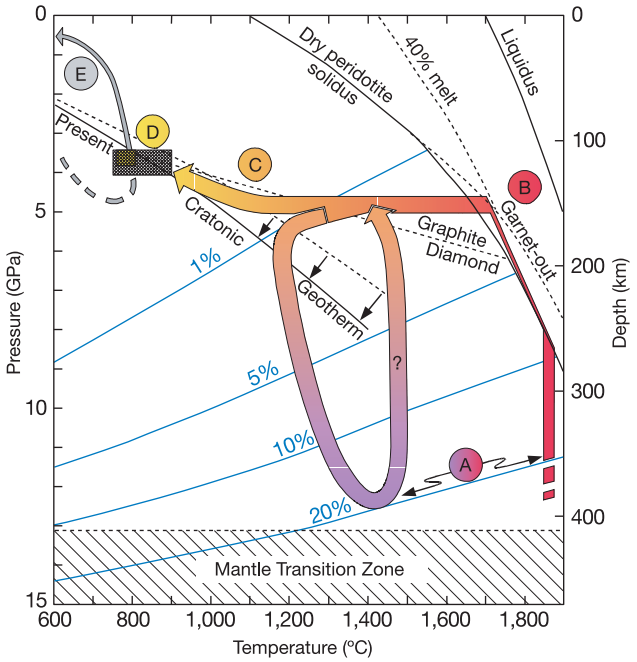

Figure 3 | Pressure–temperature diagram that schematically portrays the potential evolution of the Otrøy peridotites. Model 1 (red-orange-yellow path) requires near-isothermal decompression from depths at which the mantle contains >19% majorite in garnet (A). Extensive polybaric melting (>30%) in the Archaean continued until the mantle with garnet in the residue reached the base of the overlying lithosphere (~150 km, B). Residua were stored and cooled towards the continental geotherm in the Proterozoic. Further decompression associated with the Svecofennian or Gothian orogeny cooled the peridotites further along the cooling continental geotherm, preserving the 1.4-Gyr-ago Nd mineral cooling age (C). Model 2 (red-orange-blue-yellow path) shows that after Archaean melting, residual peridotites are subducted to at least the Mantle Transition Zone and stored until thermal equilibration resulted in buoyancy-driven upwelling. Subsolidus upwelling took the peridotites to the base of the lithosphere (B-A-C) where cooling produced the 1.4-Gyr-ago Nd mineral cooling age (C). In both models further cooling until the Phanerozoic resulted in pressure–temperature conditions in equilibrium with the present continental geotherm (D). Final peridotite exhumation to the surface occurred during the Caledonian continent–continent collision along the grey path (E)[4,31]. Rectangles represent equilibrated pressure–temperature conditions for garnet websterite lenses (grey cross-hatched) at Ugelvik (Otrøy) and Bardane (Fjørtoft)[6,7] and garnetites (yellow, see Supplementary Notes). Thin blue lines illustrate molar majorite components in solid solution with garnet[22]. The curve labelled 'Garnet-out' indicates the stability of garnet in peridotite below this curve[32].

minerals in orogenic peridotites does not necessarily record conditions of deep continental subduction as recently argued[6,10,11].

The initial Nd isotope ratio of the mineral isochron, 0.5476 (Supplementary Table 2, Supplementary Fig. 1) is extremely radiogenic compared to mantle compositions at 1.4 Gyr BP ($\epsilon Nd_{(1.4\,Gyr\,BP)} = +719$). Nd model ages calculated relative to a chondritic evolution of the mantle are 2.9 Gyr BP and 2.5 Gyr BP for olivine-bearing and olivine-absent garnetite, respectively (Supplementary Table 2). These model ages indicate that the highly depleted garnet peridotites were formed in the Archaean era. Archaean melting of the garnet peridotites is also supported by a whole-rock Re–Os model age (3.3 Gyr BP) from Otrøy[28]. The Otrøy peridotites therefore appear to be the first reported case of orogenic peridotites produced by extensive melt depletion entirely in the garnet stability field during the Archaean era.

There are two geodynamic models for SCLM formation that potentially explain the occurrence of peridotites derived from the Mantle Transition Zone at Otrøy. The simplest option (model 1, red-orange-yellow path in Fig. 3) is that Archaean adiabatic upwelling of mantle from the Mantle Transition Zone led to extensive melting and majorite exsolution. Melting stopped when the peridotites were underplated and accreted beneath an Archaean craton at depths of ~150 km. Over the next >1.0 Gyr the new SCLM cooled slowly but remained above the Nd closure temperature for clinopyroxene (~1,100 °C; ref. 19). Cooling below 1,100 °C occurred at 1.4 Gyr BP perhaps related to the Svecofennian or Gothian orogeny. The peridotites remained in the SCLM until exhumation 1.0 Gyr later during the continent–continent collision of the Caledonian orogeny.

A more complex alternative applies if the majorite formation postdates the melting (model 2, red-orange-blue-yellow path in Fig. 3). After hot upwelling, deep melting and accretion in the Archaean, part of the lower lithosphere was subducted, or delaminated, sinking to the Mantle Transition Zone accompanied by majorite formation. The low Fe peridotite residua subsequently underwent thermal equilibration and became buoyant[29], rising in a subsolidus upwelling to underplate existing SCLM in the Mid-Proterozoic, accompanied by majorite exsolution. This decompression could not involve partial melting, which would disrupt the Archaean Nd–Os isotope systematics.

Important implications of both models are that: (1) ultrahigh-pressure minerals in orogenic peridotites may be relicts that are not evidence for deep continental subduction and (2) deep asthenospheric underplating could form highly depleted SCLM with substantial amounts of garnet in the residue. We prefer the simplicity of model 1, but the more complex history of model 2 cannot be ruled out and indeed has been reproduced in numerical studies of early mantle convection[30]. Model 2 implies that cratonic lithosphere retains the ancient isotopic signature of lithosphere that has been recycled back into the convecting mantle.

A fundamental characteristic of the Otrøy peridotites is that they preserve high Mg/Si ratios, low Ca/Al ratios (almost no clinopyroxene but 5–20% garnet) and relatively enriched heavy REE. These are all characteristics inferred for the source of Al-depleted komatiites[25].

METHODS

Major elements. Mineral major-element compositions were determined by electron microprobe analysis (EMPA) at Utrecht University (JEOL JXA8600, 15 kV, 20 nA, 30 s counting time in wavelength-dispersive spectrometry mode, correction for atomic number, X-ray absorption and fluorescence by using the ZAF routine, and external calibration against international standards).

Rare earth elements. Mineral REE concentrations were measured in garnet and clinopyroxene needles (sample DS0297 and DS0298) by secondary ion mass spectrometry (SIMS) using a Cameca IMS 4f ion microprobe at CNR-IGG (Pavia). Owing to the small size of clinopyroxene exsolution, we used a $^{16}O^-$ primary-ion current intensity of 1.5–3.5 nA. We used energy filtering (−100 V offset, 50 eV energy bandwidth). Data was acquired in five cycles using counting times up to 125 s each for $^{139}La^+$, $^{140}Ce^+$, $^{146}Nd^+$ and $^{149}Sm^+$, 100 s each for $^{151}Eu^+$, $^{158}Gd^+$, $^{163}Dy^+$, $^{167}Er^+$, $^{89}Y^+$ and $^{174}Yb^+$, and 15 s for $^{30}Si^+$. Calibration standards are the following: KAUG (Kakanui augite, New Zealand), KH1 (Kilbourne Hole clinopyroxene megacryst), MNAG (pyrope megacryst from Monastery Mine, South Africa) and KAKG (pyrope megacryst from Kakanui). Precision and accuracy of the method (tested on the standards) are ~10–20% at low p.p.m. concentrations. Below 1 p.p.m., precision is constrained by (Poisson) counting statistics and worsens to several tens of per cent. Under the adopted experimental conditions, La and Ce contents in garnet are comparable to detection limits for light REE.

Laser ablation inductively coupled mass spectrometry (LA-ICP-MS) was used at Utrecht University to measure mineral REE contents in garnet and clinopyroxene from the olivine-absent garnetite (sample DS0298) and in two porphyroclastic matrix garnets (from sample DS0213 and DS0289). The system comprises a GeoLas 200Q and a Micromass Platform ICP (193 nm excimer, beam diameter 120 μm, 10 Hz, 20 J cm^{-2}). Samples were ablated for 90–120 s per spot with signal integration over >60 s. Internal calibration was performed using Ca (EMPA) and external calibration was against the NIST SRM 612 glass standard. Gd was corrected for PrO interference.

Isotope geochemistry. Garnet and intercrystalline clinopyroxene were separated by hand picking, leached in warm HCl (1 M) and warm HNO_3 (1.4 M) each for 30 min, spiked and dissolved in hot concentrated HF and HNO_3. Sm and Nd were separated using standard ion exchange procedures. Sm and Nd abundances were determined by isotope dilution using a mixed 148/150 spike and analysed as metals by thermal ionisation mass spectrometry (TIMS) at the Vrije Universiteit Amsterdam using a Finnigan MAT 262. Nd isotope ratios on unspiked aliquots were measured as oxides. Replicate analysis of the La Jolla international standard yield 0.511863 ± 9 ($n = 12$).

Volume estimates. Photographs of back-scattered electron images and a high-resolution scanned thin section were contrast-enhanced using the two-dimensional analysis software 'analySIS' (Soft Imaging System; http://www.soft-imaging.net/). Threshold detections were applied to areas up to 2.1 mm^2 for intracrystalline pyroxene needles and up to 31 cm^2 for interstitial pyroxene (corresponding to the whole sample surface shown in Fig. 1e), and checked and corrected by hand. The resulting proportions of surface percentage of pyroxene and garnet were assumed to be equal to the proportion of volume percentage between the exsolved phases.

Received 1 November 2005; accepted 13 February 2006.

1. Griffin, W. L. *et al.* Layered mantle lithosphere in the Lac de Gras area, Slave Craton: composition, structure and origin. *J. Petrol.* **40,** 705–727 (1999).
2. Pearson, D. G., Canil, D. & Shirey, S. B. in *Treatise on Geochemistry, Vol. 2: The Core and Mantle* (eds Holland, H. D. & Turekian, K. K.) 171–275 (Elsevier, Oxford, 2003).
3. Stachel, T., Viljoen, K. S., Brey, G. & Harris, J. W. Metasomatic processes in lherzolitic and harzburgitic domains of diamondiferous lithospheric mantle: REE in garnet from xenoliths and inclusions in diamonds. *Earth Planet. Sci. Lett.* **159,** 1–12 (1998).
4. Brueckner, H. K. & Medaris, L. G. A general model for the intrusion and evolution of 'mantle' garnet peridotites in high-pressure and ultra-high-pressure terranes. *J. Metamorph. Geol.* **18,** 123–133 (2000).
5. Dobrzhinetskaya, L. F. *et al.* Microdiamonds in high-grade metamorphic rocks from the Western Gneiss Region, Norway. *Geology* **23,** 597–600 (1995).
6. Brueckner, H. K., Carswell, D. A. & Griffin, W. L. Paleozoic diamonds within a Precambrian peridotite lens in UHP gneisses of the Norwegian Caledonides. *Earth Planet. Sci. Lett.* **203,** 805–816 (2002).
7. Van Roermund, H. L. M., Carswell, D. A., Drury, M. R. & Heijboer, T. C. Microdiamonds in a megacrystic garnet websterite pod from Bardane on the island of Fjørtoft, western Norway: Evidence for diamond formation in mantle rocks during deep continental subduction. *Geology* **30,** 959–962 (2002).
8. Van Roermund, H. L. M. & Drury, M. R. Ultra-high pressure (P > 6 GPa) garnet peridotites in western Norway: exhumation of mantle rocks from more than 185 km. *Terra Nova* **10,** 295–301 (1998).
9. Van Roermund, H. L. M., Drury, M. R., Barnhoorn, A. & de Ronde, A. Relict majoritic garnet microstructures from ultra-deep orogenic peridotites in western Norway. *J. Petrol.* **42,** 117–130 (2001).
10. Ye, K., Cong, B. & Ye, D. The possible subduction of continental material to depth greater than 200 km. *Nature* **407,** 734–736 (2000).
11. Song, S., Zhang, L. & Niu, Y. Ultra-deep origin of garnet peridotite from the North Qaidam ultrahigh-pressure belt, Northern Tibetian Plateau, NW China. *Am. Mineral.* **89,** 1330–1336 (2004).
12. Drury, M. R. *et al.* Emplacement of deep upper-mantle rocks into cratonic lithosphere by convection and diapiric upwelling. *J. Petrol.* **42,** 131–140 (2001).
13. Carswell, D. A. Possible primary upper mantle peridotite in Norwegian basal gneiss. *Lithos* **1,** 322–355 (1968).

14. Carswell, D. A. Garnet pyroxenite lens within Ugelvik layered garnet peridotite. *Earth Planet. Sci. Lett.* **20,** 347–352 (1973).
15. Dobrzhinetskaya, L. F. *et al.* Precipitation of pyroxenes and olivine from majoritic garnet: simulation of peridotite exhumation from great depth. *Terra Nova* **16,** 325–330 (2004).
16. Haggerty, S. E. & Sautter, V. Ultradeep (greater than 300 kilometers), ultramafic upper mantle xenoliths. *Science* **248,** 993–996 (1990).
17. Burgess, S. R. & Harte, B. Tracing lithosphere evolution through the analysis of heterogeneous G9–G10 garnets in peridotite xenoliths, II: REE chemistry. *J. Petrol.* **45,** 609–634 (2004).
18. Schmidberger, S. S. & Francis, D. Constraints on the trace element composition of the Archean mantle root beneath Somerset Island, Arctic Canada. *J. Petrol.* **42,** 1095–1117 (2001).
19. Van Orman, J. R., Grove, T. L., Shimizu, N. & Layne, G. D. Rare earth element diffusion in a natural pyrope single crystal at 2.8 GPa. *Contrib. Mineral. Petrol.* **142,** 416–424 (2002).
20. Johnson, K. T. M. Experimental determination of partition coefficients for rare earth and high-field-strength elements between clinopyroxene, garnet, and basaltic melt at high pressures. *Contrib. Mineral. Petrol.* **133,** 60–68 (1998).
21. Fei, Y. & Bertka, C. M. in *Mantle Petrology: Field Observations and High-Pressure Experimentation* (eds Fei, Y., Bertka, C. M. & Mysen, B. O.) Spec. Publ. No. 6, 189–207 (The Geochemical Society, Houston, 1999).
22. Gasparik, T. *Phase Diagrams for Geoscientists—An Atlas of the Earth's Interior* (Springer, Berlin, 2003).
23. Hellebrand, E., Snow, J. E., Hoppe, P. & Hofmann, A. W. Garnet-field melting and late stage refertilization in 'residual' abyssal peridotites from the central indian ridge. *J. Petrol.* **43,** 2305–2338 (2002).
24. Ionov, D. Chemical variations in peridotite xenoliths from Vitim, Siberia: inferences for REE and Hf behaviour in the garnet-facies upper mantle. *J. Petrol.* **45,** 343–367 (2004).
25. Herzberg, C. Geodynamic information in peridotite petrology. *J. Petrol.* **45,** 2507–2530 (2004).
26. Takahashi, E. Speculations on the Archean mantle: missing link between komatiite and depleted garnet peridotite. *J. Geophys. Res.* **95,** 15941–15954 (1990).
27. Green, H. W. II, Dobrzhinetskaya, L. & Bozhilov, K. N. Mineralogical and experimental evidence for very deep exhumation from subduction zones. *J. Geodynam.* **30,** 61–76 (2000).
28. Beyer, E. E., Brueckner, H. K., Griffin, W. L., O'Reilly, S. Y. & Graham, S. Archean mantle fragments in Proterozoic crust,Western Gneiss Region, Norway. *Geology* **32,** 609–612 (2004).
29. Ringwood, A. E. Role of the transition zone and 660 km discontinuity in mantle dynamics. *Phys. Earth Planet. Inter.* **86,** 5–24 (1994).
30. De Smet, J. H., Van den Berg, A. P. & Vlaar, N. J. Early formation and long-term stability of continents resulting from decompression melting in a convecting mantle. *Tectonophysics* **322,** 19–33 (2000).
31. Terry, M. P., Robinson, P. & Krogh Ravna, E. J. Kyanite eclogite thermobarometry and evidence for thrusting of UHP over HP metamorphic rocks, Nordøyane, Western Gneiss Region, Norway. *Am. Mineral.* **85,** 1637–1650 (2000).
32. Walter, M. J. in *Treatise on Geochemistry, Vol. 2: The Core and Mantle* (eds Holland, H. D. & Turekian, K. K.) 363–394 (Elsevier, Oxford, 2003).

Supplementary Information is linked to the online version of the paper at www.nature.com/nature.

Acknowledgements This project was initiated during the NWO-PIONIER project of M.R.D. and subsequently funded by the Utrecht University Institute of Geodynamic Research. Electron microscopy was conducted at the Electron Microscopy Utrecht centre. The National Research Council of Italy is acknowledged for funding the SIMS laboratory at CNR-IGG (Pavia). The isotope and LA-ICP-MS facilities at Vrije Universiteit and Universiteit Utrecht are supported by the Netherlands Organisation for Scientific Research. We thank M. Røberg and T. Wilhelmsen for providing appropriate samples. P. J. O'Brien is thanked for suggestions that have led to improvements of this paper. Thanks also to H. K. Brueckner, D. A. Carswell, H. Green II, A. Scherstén and W. van Westrenen.

Author Information Reprints and permissions information is available at npg.nature.com/reprintsandpermissions. The authors declare no competing financial interests. Correspondence and requests for materials should be addressed to D.S. (spengler@geo.uu.nl).